

Original Paper

Control of Insulin Release by Transient Receptor Potential Melastatin 3 (TRPM3) Ion Channels

Alexander Becker^a Stefanie Mannebach^a Ilka Mathar^a Petra Weissgerber^a
Marc Freichel^{b,c} Asia Perveen Loodin^a Claudia Fecher-Trost^a Anouar Belkacemi^a
Andreas Beck^a Stephan Ernst Philipp^a

^aExperimental and Clinical Pharmacology and Toxicology / Center for Molecular Signalling (PZMS), Saarland University, Homburg, Germany, ^bPharmakologisches Institut, Ruprecht-Karls-Universität Heidelberg, Heidelberg, Germany, ^cDZHK (German Centre for Cardiovascular Research), partner site Heidelberg/Mannheim, Heidelberg, Germany

Key Words

Transient receptor potential M3 channels (TRPM3) • Calcium • Glucose-stimulated insulin secretion • CRISPR/Cas • INS-1 • *Trpm3* knockout

Abstract

Background/Aims: The release of insulin in response to increased levels of glucose in the blood strongly depends on Ca²⁺ influx into pancreatic beta cells by the opening of voltage-gated Ca²⁺ channels. Transient Receptor Potential Melastatin 3 proteins build Ca²⁺ permeable, non-selective cation channels serving as pain sensors of noxious heat in the peripheral nervous system. TRPM3 channels are also strongly expressed in pancreatic beta cells that respond to the TRPM3 agonist pregnenolone sulfate with Ca²⁺ influx and increased insulin release. Therefore, we hypothesized that in beta cells TRPM3 channels may contribute to pregnenolone sulfate- as well as to glucose-induced insulin release. **Methods:** We used INS-1 cells as a beta cell model in which we analysed the occurrence of TRPM3 isoforms by immunoprecipitation and western blotting and by cloning of RT-PCR amplified cDNA fragments. We applied pharmacological as well as CRISPR/Cas9-based strategies to analyse the interplay of TRPM3 and voltage-gated Ca²⁺ channels in imaging experiments (FMP, Fura-2) and electrophysiological recordings. In immunoassays, we examined the contribution of TRPM3 channels to pregnenolone sulfate- and glucose-induced insulin release. To confirm our findings, we generated beta cell-specific *Trpm3*-deficient mice and compared their glucose clearance with the wild type in glucose tolerance tests. **Results:** TRPM3 channels triggered the activity of voltage-gated Ca²⁺ channels and both channels together contributed to insulin release after TRPM3 activation. *Trpm3*-deficient INS-1 cells lacked pregnenolone sulfate-induced Ca²⁺ signals just like the pregnenolone sulfate-induced insulin release. Both,

A. Becker and S. Mannebach contributed equally to this work.

Stephan E. Philipp

Experimental and Clinical Pharmacology and Toxicology / Center for Molecular Signalling (PZMS),
Saarland University, Homburg (Germany)
Tel. 0049-6841-1626152, Fax 0049-6841-1626402, E-Mail stephan.philipp@uks.eu

glucose-induced Ca^{2+} signals and the glucose-induced insulin release were strongly reduced. Accordingly, *Trpm3*-deficient mice displayed an impaired decrease of the blood sugar concentration after intraperitoneal or oral administration of glucose. **Conclusion:** The present study suggests an important role for TRPM3 channels in the control of glucose-dependent insulin release.

© 2020 The Author(s). Published by
Cell Physiol Biochem Press GmbH&Co. KG

Introduction

The major function of pancreatic beta cells is the supply of insulin in response to increased blood glucose levels. After glucose uptake into the beta cell, the glycolytic increase of ATP induces the closure of ATP-dependent potassium channels leading to membrane depolarization, opening of voltage-gated Ca^{2+} channels (CaV), and increase of the concentration of cytosolic Ca^{2+} ($[\text{Ca}^{2+}]_{\text{cyt}}$), which in turn triggers the fusion of insulin-containing vesicles with the plasma membrane and the release of insulin into the blood [1].

Thus, ATP-dependent potassium channels and CaV channels serve as main mediators of insulin release, but additional channel proteins and among them, channels of the transient receptor potential (TRP) protein family participate in this process [1, 2]. For example, glucose-induced oscillations of cytosolic Ca^{2+} had a reduced frequency in pancreatic islets from *Trpm5* knockout mice which was accompanied by reduced glucose-induced insulin release and impaired glucose tolerance [3]. Similarly, TRPM2-deficient pancreatic islet cells displayed reduced Ca^{2+} signals as well as impaired insulin secretion in response to glucose and glucagon-like peptide 1 [4]. TRPM3 channels are activated by the neurosteroid pregnenolone sulfate (PS, [5]) and induce a strong increase of $[\text{Ca}^{2+}]_{\text{cyt}}$ [6-9]. In neurons - where they serve as pain sensors [10, 11] - their activity is temperature-dependent [10] and tightly controlled by G $\beta\gamma$ -subunits of G-protein coupled receptors [12-15]. The TRPM3 channel activity is enhanced by membrane phosphoinositides [16, 17]. On the other hand, it is inhibited by Ca^{2+} probably via interaction with Ca^{2+} /calmodulin [18, 19]. The identification of two phosphatidylinositol 4,5-bisphosphate (PIP₂) binding sites overlapping with calmodulin-binding regions suggested a balanced control of TRPM3 channels by Ca^{2+} /calmodulin and phosphoinositides [20].

We could show that TRPM3 channels are expressed in pancreatic beta cells [5], where they establish an influx pathway for Zn^{2+} , an ion that is co-released with insulin and essential for insulin secretion [21]. We proposed that TRPM3 channels may also contribute to glucose-induced insulin release since we found that pancreatic islets secrete insulin in response to PS [5]. In line with this idea, TRPM3-deficient pancreatic islets did not longer show PS-induced insulin release [22].

Here, we use TRPM3-deficient INS-1 insulinoma cells, to analyse the role of TRPM3 channels in insulin secretion. We demonstrate that the PS-induced insulin release originates exclusively from the activation of TRPM3. The TRPM3 activity alone is already sufficient to trigger insulin release and in addition activates voltage-gated Ca^{2+} influx. Most importantly, we show that TRPM3 channels also contribute to the glucose-induced increase of $[\text{Ca}^{2+}]_{\text{cyt}}$ and the glucose-induced insulin secretion. Consistently, TRPM3-deficient mice displayed delayed clearance of blood glucose in response to a glucose load.

Materials and Methods

Cell culture and reagents

INS-1 cells [23] were cultured in RPMI 1640 medium (Gibco) supplemented with 10 % (v/v) fetal calf serum, 1 mM sodium pyruvate, 1 mM 4-(2-hydroxyethyl)-1-piperazineethanesulfonic acid (HEPES), 50 μM β -mercaptoethanol, 100 U/ml penicillin and 100 $\mu\text{g}/\text{ml}$ streptomycin. HEK α 2 cells [24] were cultured in Minimum Essential Medium (Gibco) containing 10 % fetal calf serum, 100 U/ml penicillin, 100 $\mu\text{g}/\text{ml}$ streptomycin, and 500 $\mu\text{g}/\text{ml}$ geneticin. Cells were cultured at 37°C and 5 % CO_2 in a humidified atmosphere

and passaged after trypsinization 1-2 times a week. 100 mM stock solutions of pregnenolone sulfate, hesperetin, isosakuranetin, and verapamil were prepared in DMSO and stored at -20°C.

Immunoprecipitation and western blotting

Immunoprecipitations were performed as described [25] using monoclonal anti-TRPM3 antibodies from rat [5] and affinity-purified polyclonal anti-TRPM3 antibodies from rabbit directed against the rat TRPM3 epitope QEKEPEEPEKPTKEK [6]. Rat immunoglobulin G (IgG) served as a control for the specificity of the immunoprecipitation and anti-calnexin antibodies (ADI-SPA-865-D, Enzo Life Sciences) were used to detect calnexin as a loading control in western blots. Labelled proteins were visualized using horseradish peroxidase-labelled secondary antibodies and the Western Lightning Chemiluminescence Reagent Plus (PerkinElmer).

*Identification of *Trpm3* transcripts in INS-1 cells*

5 µg total RNA from rat brain or INS-1 cells were reverse transcribed using SuperScript 2 Reverse Transcriptase (Invitrogen). Fragments encoding entire TRPM3 proteins were amplified using the oligonucleotide primers A (5' ATG GGC AAG AAG TGG AGG GAC), B (5' ATG CCA GGG CCG TGG GGG AC), C (5' CTG CAG AAC TTT GAA CTC CAG C), D (5' TCC TGC AAC ACA CGG GAA GAT G) and the Expand Long Template PCR System (Roche) according to the manufacturer's advice. For amplification of cDNA fragments < 1000 bp we used 100 ng total RNA for each reaction, the SuperScript One-Step RT-PCR System (Thermo Fisher Scientific), and the following oligonucleotide primers: E (5' GAA TCG GTC AAG GGG TTC CAG), F (5' ACT GCT GCC CGT AAA TAA AGA TC), G (5' CCC AAT GAG GAG CCA TCT TGG) and H (5' CCA TGA TGG CTG GCA CAA TCC). Amplicons were cloned in pBluescript KS⁺ and sequenced on both strands.

*CRISPR/Cas9-mediated knockout of the *Trpm3* gene in INS-1 cells*

To identify appropriate gRNA target sequences for editing of the *Trpm3* gene we used the freely available online programs CRISPR.MIT.EDU [26] and E-CRISP [27]. In addition, Cas-OFFinder was used to identify possible off-target sequences [28]. To allow the identification of mutations, each of the identified sequences 5' GA GCC TGG ATC TTC ACT GGA GGG (M3gRNA-1), 5' GA CCC CTC CAG TGA AGA TCC AGG (M3gRNA-2) and 5' GT ACT TCG TCA TCA TTA TGC TGG (M3gRNA-3) contained a restriction recognition site which overlapped the Cas9 cleavage site three nucleotides upstream of the protospacer adjacent motif. The target sequences were inserted into the vector pGS-U6-gRNA (Genscript), and INS-1 cells were co-transfected together with pcDNA3.3-Cas9-2A-eGFP, encoding the Cas9 enzyme and - linked via a 2A peptide sequence - the enhanced green fluorescent protein [29]. Three days post-transfection single green fluorescent cells were sorted into distinct wells of a 96-well plate using a MoFlo-XDP cell sorter (Beckman Coulter). Genomic *Trpm3* fragments were PCR-amplified using oligonucleotide primers I (5' CTG CAG AAC TTT GAA CTC CAG C), J (5' AGT AAA GTC ACT CCT CCT ATG C), K (5' GTA TTC AGT ATG CGG ACA TCC G) and L (5' CCA AGA TGG CTC CTC ATT GGG; Fig. 3a). Amplicons were analysed by hydrolysis with TspR1 (M3gRNA-1, 213/96 bps) or Mbo1 (M3gRNA-2, 226/83 bps) or Msl1 (M3gRNA-3, 153/74 bps) and by sequencing of both strands (Fig. 3a).

Insulin secretion

After trypsinization, INS-1 cells were counted using an automated cell counter (Countess, Invitrogen) and 10⁵ cells were seeded into one well of a poly-L-lysine coated 96-well plate each (Falcon). After three days, the medium was removed and cells were equilibrated in glucose-free Krebs Ringer bicarbonate HEPES buffer (KRBH; 135 mM NaCl, 3.6 mM KCl, 5 mM NaHCO₃, 0.5 mM NaH₂PO₄, 0.5 mM MgCl₂, 1.5 mM CaCl₂, 10 mM HEPES, 0.1 % (w/v) BSA, 290 ± 5 mosm/kg, pH 7.4) for 30 minutes at 37°C and 5 % CO₂. Thereafter, the solution was removed and cells were incubated for 30 or 60 minutes in 180 µl KRBH containing additional agents as indicated in the figure legends. Plates were centrifuged at 200×g for 5 min and 60 - 90 µl of the supernatants were removed for analysis. Samples were either analysed directly or stored at -80°C for no longer than one month. The insulin concentration in 5 µl supernatant was determined with an AlphaLISA Assay (AL350, PerkinElmer) according to the manufacturer's protocol. Samples were measured with an EnSight multimode plate reader (PerkinElmer) and data was acquired with the associated Kaleido software (PerkinElmer).

Fluorescent Ca²⁺ measurements

The measurements of the cytosolic Ca²⁺ concentration were performed essentially as described [24]. In brief, cells were seeded on poly-L-lysine coated glass coverslips submerged in 2 ml medium. After 2-3 days, cells were loaded with 5 μM fura-2-acetoxymethyl ester (fura-2AM; Fisher Scientific) supplemented in KRBH for 30 minutes at 37°C and 5% CO₂. Cells were washed twice with KRBH and analysed in a perfusion chamber (Warner Instruments, Hamden CT) with continuous perfusion of 1 ml/min at room temperature. Alternatively, measurements were performed in 300 μl KRBH in an open chamber and cells were stimulated by the addition of 300 μl of appropriate solutions. The fluorescence was excited at 340 nm and 380 nm for 20 ms each every three seconds and emissions were recorded at λ >440 nm with a CCD camera. Fluorescence ratios of individual cells were calculated after background subtraction using Till Vision software (TILL Photonics).

Fluorescent membrane potential measurements

Fluorescent membrane potential measurements were performed essentially as described [30]. In brief, the FLIPR membrane potential-sensitive dye (FMP) was dissolved in a buffer containing 140 mM NaCl, 2.8 mM KCl, 2 mM MgCl₂, 1 mM CaCl₂, 10 mM HEPES, 10 mM glucose, pH 7.4 or in high potassium buffer containing 70 mM NaCl, 70 mM KCl, 2 mM MgCl₂, 1 mM CaCl₂, 10 mM HEPES, 10 mM glucose, pH 7.4. Both solutions were mixed at equal amounts to reach 36.4 mM KCl. Pregnenolone sulfate and isosakuranetin were added to reach final concentrations as indicated. Measurements were performed at an Axiovert 200M microscope (Zeiss) equipped with a 20x Fluor objective (Zeiss), a polychrom V monochromator (TILL Photonics, Martinsried, Germany), and an IXon CCD camera (Andor). FMP was excited by 530 nm light and the emission was detected at 624 ± 40 nm.

Electrophysiological recordings

Whole-cell currents were recorded from wild-type and TRPM3-deficient INS-1 cells at an Axiovert 135 M microscope (Zeiss) equipped with a 40x LD Achromplan objective (Zeiss), using a computer-controlled EPC-9 patch clamp amplifier (HEKA Electronics, Lambrecht, Germany) and the PatchMaster software (HEKA). Patch pipettes were pulled from glass capillaries GB150T-8P (Science Products, Hofheim, Germany) at a PC-10 micropipette puller (Narishige, Tokyo, Japan) and had resistances between 3 and 4 MΩ when filled with internal (pipette) solution containing (in mM) 120 Cs-glutamate, 8 NaCl, 1 MgCl₂, 10 HEPES, 10 Cs-BAPTA (1,2-bis(2-aminophenoxy)ethane-N,N,N',N'-tetraacetic acid); pH adjusted to 7.2 with CsOH. The external solution comprised (in mM) 140 NaCl, 2 MgCl₂, 1 CaCl₂, 10 HEPES, 10 glucose, 10 μM verapamil; pH adjusted to 7.2 with NaOH. For application 100 μM pregnenolone sulfate (PS) were added and administered directly onto the patch clamped cell via a wide-tipped patch pipette. All solutions had an osmolality between 285 and 305 mosmol/kg. For current measurements, 400 ms voltage ramps spanning from -100 to +100 mV were applied every 2 s from a holding potential (V_h) of 0 mV. Currents were filtered at 2.9 kHz and digitized at 400 μs intervals. All voltages were corrected for a 10 mV liquid junction potential. Capacitive currents and series resistance were determined and corrected before each voltage ramp using the automatic capacitance compensation of the EPC-9. Current amplitudes at -80 and 80 mV were extracted from current ramps and plotted versus time. All currents were normalized to the cell capacitance as a measure of the cell size to calculate current densities (pA/pF).

Generation of beta cell-specific Trpm3 knockout mice

Mice carrying an L3F2 allele (Fig. 5a) were generated as described [15]. Mice with a floxed *Trpm3* allele (L2) in which exon 24 is flanked by loxP sequences (Fig. 5a) were obtained by mating L3F2 mice with EIIa-Cre deleter mice [31]. Due to the low EIIa promoter activity, the Cre-positive offspring carried a genetic mosaic of three *Trpm3* alleles including the floxed *Trpm3* (L2) allele (Fig. 5a). Mating of mosaic mice that carried the floxed *Trpm3* allele in their germ cells with wild-type animals produced a heterozygous *Trpm3*^{+/floxed} offspring which was further bred to obtain *Trpm3*^{flox/flox} animals. RIP-Cre mice expressing the Cre recombinase under the control of the rat insulin promoter [32] were crossed with *Trpm3*^{-/-} mice [15] and the *Trpm3*^{-/-}, RIP-Cre positive (RIP-Cre⁺) offspring was mated with *Trpm3*^{flox/flox} animals to obtain *Trpm3*^{-/-flox}, RIP-Cre⁺ animals which were TRPM3-deficient exclusively in pancreatic beta cells. In experiments, their *Trpm3*^{-/-flox}, RIP-Cre negative (RIP-Cre⁻) littermates served as controls.

Glucose tolerance test

Blood glucose concentrations of male mice were determined at an age of 20 to 21 weeks each after 12 - 14 hours of fasting and 15, 30, 60, and 120 min after intraperitoneal (IP) or oral administration of 2 g glucose/kg body weight. 5 - 10 μ l of blood were collected after a single incision at the tail end and analysed using a blood sugar measuring device (FreeStyle, Disetronic). *Trpm3*^{-flox}, RIP-Cre⁺ and *Trpm3*^{-flox}, RIP-Cre⁻ control mice were examined in parallel.

Data processing and statistics

Data of insulin measurements were processed using the GraphPad Prism software and are depicted in scattergrams together with their mean values. Ratio data from fluorescent Ca²⁺ measurements were plotted as individual curves together with their mean value, or mean values only, both together with the corresponding standard error of the mean (SEM) using OriginPro. One-way analysis of variance (one-way ANOVA) combined with Bonferroni's multiple comparison test was performed to test the statistical significance of differences between samples. In glucose tolerance experiments data were tested for their statistical significance using two-way repeated measures ANOVA with Bonferroni post-hoc test. In the figures, the statistical significance of differences between samples is indicated by asterisks with *p < 0.05, **p < 0.01, ***p < 0.001 and ns = not significant.

Results

INS-1 cells provide a suitable beta cell model to study the role of TRPM3 in insulin release

To analyse the role of TRPM3 channels in pancreatic beta cells, we used rat insulinoma cells of the line INS-1, which upon addition of glucose or the TRPM3 agonist pregnenolone sulfate (PS) raise [Ca²⁺]_{cyt} and release insulin [5, 23, 33]. Fig. 1a shows, that the cells responded to the application of glucose and PS with enhanced insulin release in a concentration-dependent manner and that the PS-induced release was additive both at low and high glucose concentrations. Furthermore, PS stimulated the insulin release also in the absence of glucose (Fig. 2h). Immunoprecipitation experiments using a combination of monoclonal (mab) and polyclonal (pab) anti-TRPM3 antibodies confirmed the presence of TRPM3 proteins in INS-1 cells (Fig. 1b, [5]).

Since the properties of TRPM3 isoforms widely diverge with regard to functionality and Ca²⁺ permeability [8, 24, 34], we next asked, which TRPM3 variants are present in INS-1 cells. For that purpose, we analysed the rat *Trpm3* gene and the *Trpm3* transcriptome in INS-1 cells in more detail (Fig. 1c-f). The rat *Trpm3* gene is located on chromosome 1q51, encompasses at least 870 kb, and displays an exon-intron structure very similar to the genes from mouse and man (Fig. 1c). For transcriptome analysis, mutually exclusive *Trpm3* transcripts starting with exon 1 (*Trpm3 α* or exon 2 (*Trpm3 β* [34] were amplified using sense oligonucleotide primers A, B, or C (as control) each in combination with the antisense primer D, matching to the very last coding nucleotides of the *Trpm3* gene (Fig. 1d). Amplicons > 5 kb were obtained with each of the primer combinations from brain, suggesting the presence of both α - and β -variants. From INS-1 RNA however, no fragments were amplified with primer combination B/D (n = 4), indicating the absence of TRPM3 β -variants in INS-1-cells. A/D- amplicons from INS-1 cells were cloned and sequenced (Fig. 1e). Among 27 transcripts analysed, we found twelve that corresponded to the isoform TRPM3 α 2 from mouse [24]. Further three and seven transcripts encoded the isoforms TRPM3 α 3 and TRPM3 α 6, respectively. The encoded proteins differed by only 13 single amino acid exchanges and displayed > 99 % amino acid sequence identity to the corresponding mouse proteins. In addition, we identified four novel TRPM3 splice variants TRPM3 α 10, TRPM3 α 18, TRPM3 α 19, and TRPM3 α 20 from rat (Fig. 1e). *Trpm3 α 18* transcripts lacked rat exon 28 (133 nt) causing a frameshift and a premature translation stop of the protein. In contrast, *Trpm3 α 19*- and *Trpm3 α 20*- transcripts contained a new, thus far unknown exon 17 encoding 28 additional amino acid residues (Fig. 1c, e). Hence, the *Trpm3* gene from rat comprises in total 29 coding exons. All TRPM3 variants identified in INS-1 cells contained a domain encoded by exon 13 which is indispensable for

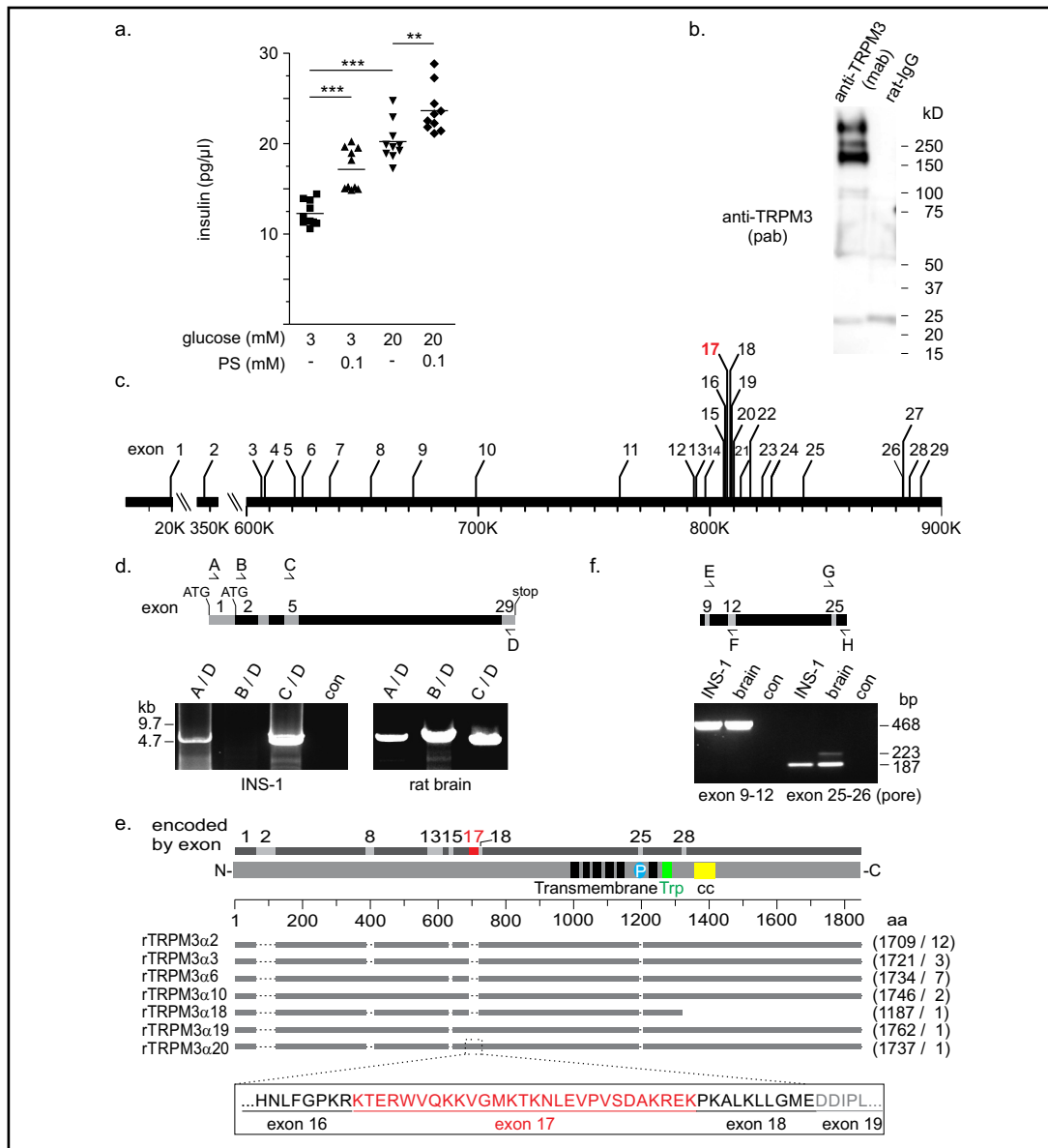


Fig. 1. Properties of INS-1 beta cells as a model to analyse the role of TRPM3 in insulin release. (a) Insulin released from INS-1 cells in the presence of 3 and 20 mM glucose and the absence and presence of 0.1 mM PS. (b) Identification of TRPM3 proteins in INS-1 cells using monoclonal anti-TRPM3-antibodies (mab) from rat for immunoprecipitation and polyclonal anti-TRPM3-antibodies (pab) for detection in a western blot. Rat immunoglobulin G (IgG) served as control. (c) Genomic organization of the rat *Trpm3* gene located on chromosome 1q51 spanning ~ 870 kb and comprising 29 exons. A newly identified exon 17 is highlighted in red. (d) Amplification of *Trpm3* transcripts by RT-PCR from INS-1 cells and rat brain. The location of the target sequences of the oligonucleotide primers A, B, C, and D within the predicted rat exons (numbers) is indicated in the diagram. Control reactions (con) without template revealed no products. (e) Schematic presentation of TRPM3 protein isoforms (grey bars) identified in INS-1 cells and scaled to their relative size with the numbers of amino acid residues (aa) and the number of identified clones indicated in brackets. Internal protein domains removed by alternative splicing are indicated as dotted lines. The protein region encoded by a newly identified exon 17 (red) is presented below. The organization of TRPM3 protein domains is shown above, with the transmembrane region including the six transmembrane domains (black rectangles), the channel pore (P), the TRP motif (Trp), and a coiled-coil region (cc) as indicated. Alternative protein-coding exons identified in mouse [24] and rat are indicated on top, with the newly identified exon 17 highlighted in red. (f) Detection of pore-coding *Trpm3* transcripts in INS-1 cells and rat brain by RT-PCR. The locations of the targets of the oligonucleotide primers G and H to amplify transcripts encoding the pore regions (exon 25-26) and of oligonucleotide primers E and F to amplify fragments common to all *Trpm3* transcripts (exon 9-12) as control are indicated.

the TRPM3 channel function (Fig. 1e [24]). Furthermore, all *Trpm3* transcripts lacked a part of exon 25 (36 nt) which encodes a longer pore loop (Fig. 1e). Long pore variants display a strongly reduced Ca^{2+} permeability and lack inhibition by monovalent cations [8]. To confirm our finding, we performed additional RT-PCR experiments using primers located in exon 25 and exon 26 upstream and downstream of the spliced sequence (Fig. 1f). In contrast to rat brain RNA, no transcripts encoding a long pore were amplified from INS-1 cells. Hence, common to all TRPM3 variants identified in INS-1 cells was the presence of a short pore loop. Suchlike variants display a fractional Ca^{2+} current of 24 % under physiological ion conditions and therefore significantly increase $[\text{Ca}^{2+}]_{\text{cyt}}$ after activation [9]. Taken together, the data showed that INS-1 cells express functional and Ca^{2+} -permeable TRPM3 channel proteins that display both a PS- and a glucose-induced insulin release. Therefore, INS-1 cells constitute an appropriate beta cell model to analyse the contribution of TRPM3 channels to insulin release.

TRPM3 channels stimulate voltage-gated Ca^{2+} channels and both channels, TRPM3 and CaV, contribute in concert to PS-induced insulin release

Next, we asked whether and how TRPM3 channels cooperate with voltage-gated Ca^{2+} channels. In the presence of the TRPM3 antagonists hesperetin [35] and isosakuranetin [36] the PS-induced increase of $[\text{Ca}^{2+}]_{\text{cyt}}$ was completely absent (Fig. 2a, d-f), showing that in INS-1 cells TRPM3 channels were active and that PS did not directly activate voltage-gated Ca^{2+} channels. Conversely, the L-type CaV-antagonist verapamil in a concentration of 50 μM did not affect the PS-induced Ca^{2+} entry through TRPM3 channels (Fig. 2b) but it inhibited completely the potassium-induced Ca^{2+} influx through voltage-gated Ca^{2+} channels (Fig. 2c) demonstrating that in INS-1 cells verapamil inhibits CaV but does not influence TRPM3 channels.

In the absence of any stimuli (control condition), we observed spontaneous Ca^{2+} oscillations in INS-1 cells that were considerably reduced after addition of verapamil but not after addition of isosakuranetin (Fig. 2d). This suggests a constitutive CaV activity in INS-1 cells. In agreement with this observation, the insulin release (in the absence of any stimulus) was strongly reduced in the presence of verapamil (Fig. 2h). Now we tested the effects of verapamil upon the PS-induced Ca^{2+} entry. The blockage of CaV channels by verapamil significantly reduced the PS-induced Ca^{2+} increase by 62 %, indicating that TRPM3 channels stimulate Ca^{2+} entry through CaV channels (Fig. 2e, f). Since the reversal potential of TRPM3 channels is close to 0 mV [5], the opening of TRPM3 channels may depolarize the cell membrane potential, which in turn may trigger the activity of voltage-gated Ca^{2+} channels. To test this hypothesis, we analysed changes of the membrane potential following PS stimulation of TRPM3 channels using the membrane potential dye FMP (Fig. 2g). Corresponding to the observed spontaneous Ca^{2+} oscillations (Fig. 2d) we found transient depolarizations of the membrane potential in some cells already in the absence of any stimuli (data not shown). In response to PS stimulation, we observed an immediate increase of the membrane potential that was absent in the presence of isosakuranetin (Fig. 2g). This finding demonstrates that the opening of TRPM3 channels raises the membrane potential which is expected to activate voltage-gated Ca^{2+} channels as a direct consequence.

On the other hand, we observed - even in the presence of verapamil - a significant Ca^{2+} -increase of 38 % after PS stimulation (Fig. 2f), demonstrating that TRPM3 channels themselves contribute significantly to Ca^{2+} entry in INS-1 cells. Accordingly, the addition of PS induced a significant release of insulin when CaV channels were blocked by verapamil (Fig. 2h). Hence, Ca^{2+} entering the cell through TRPM3 channels is sufficient to induce an insulin release from INS-1 cells. Finally, in the absence of verapamil, PS induced a further enhanced release of insulin which is most likely due to Ca^{2+} entry through both channels TRPM3 and CaV (Fig. 2h).

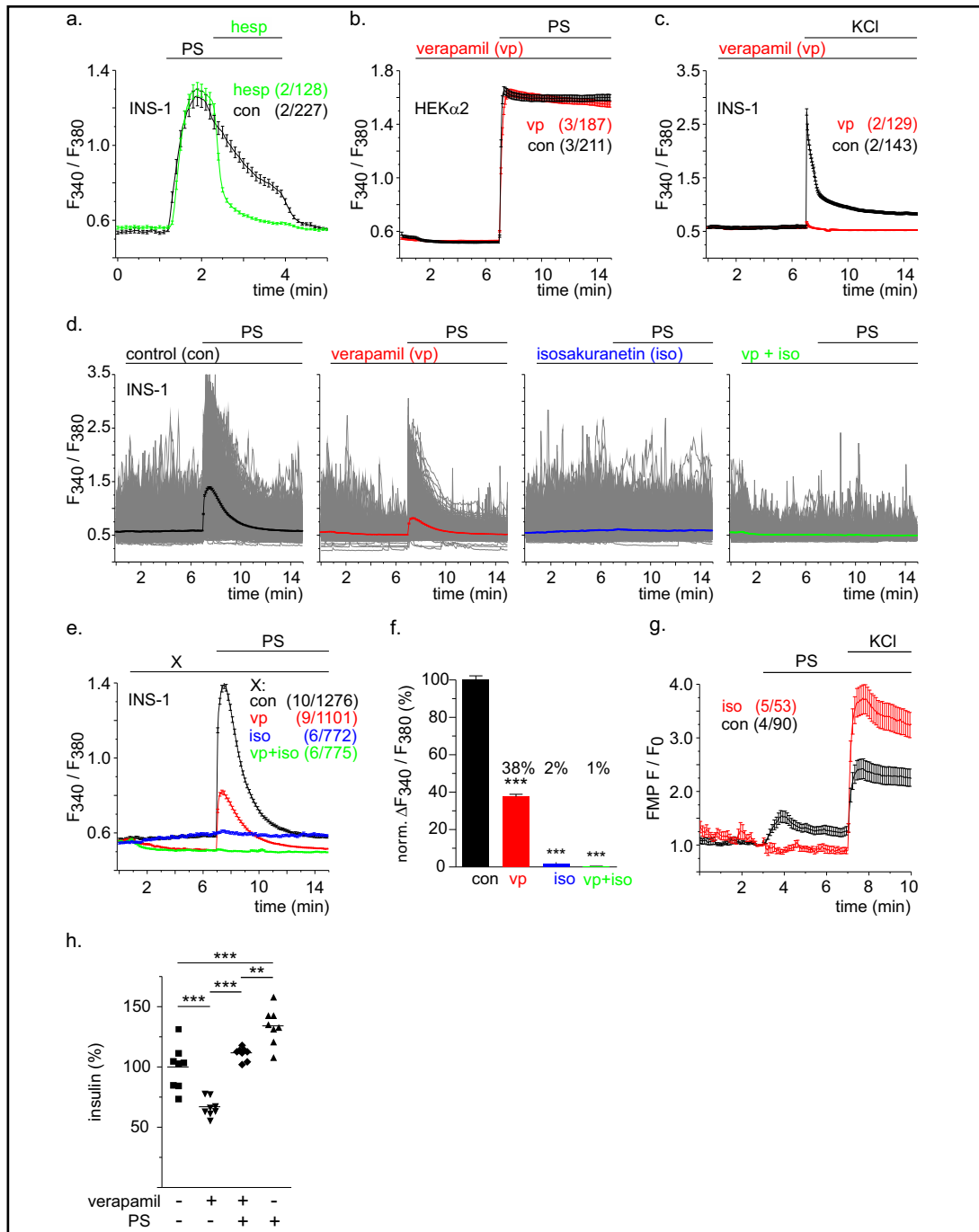


Fig. 2. TRPM3 triggers CaV activity and both channels together contribute to PS-induced insulin release. (a-f) Fura-2 fluorescence ratios measured in INS-1 cells (a, c-f) or TRPM3α2-overexpressing HEK293 cells (HEKα2, b) before and after addition of 100 μM PS or 25 mM potassium chloride (KCl) in the absence or presence of 50 μM hesperetin (hesp), 50 μM verapamil (vp), 10 μM isosakuranetin (iso) or solvent only (con) as indicated. Thick traces represent mean values (± SEM) with the numbers of experiments/cells indicated in brackets. (d) Measurements of single cells are shown in grey. (e) Summary of the experiments shown in (d). (f) Maximal increase of [Ca²⁺]_{cyt} shown in (e) before and after the addition of PS. Values were normalized to the mean of the control value and are indicated above the bars. (g) Fluorescence changes in INS-1 cells of the voltage-sensitive FLIPR dye FMP in INS-1 cells upon application of 100 μM PS or 36,4 mM KCl as control in the absence (con) and presence of 10 μM isosakuranetin (iso). Results are given as mean F / F₀ ± S.E.M. with F₀ = mean of F160 to 180 s with the numbers of experiments/cells indicated in brackets. (h) Insulin released from INS-1 cells in the absence (-) or presence (+) of 100 μM PS and/or 50 μM verapamil. Values were normalized to the mean level obtained in the absence of both compounds.

Deletion of TRPM3 channels abolishes PS-induced elevation of $[Ca^{2+}]_{cyt}$ and insulin release

To further support these findings and to exclude that PS serves TRPM3-independent actions in pancreatic beta cells we generated TRPM3-deficient INS-1 cell clones (knockout) using a CRISPR/Cas9-based strategy (Fig. 3a). To rule out off-target phenotypes, we selected three independent targets within the *Trpm3* gene. Two of them were located in exon 5, the first protein-coding exon common to all TRPM3 variants from mouse, man, and rat (Fig. 1e, [34]). The third target was located in exon 25 which encodes the pore region of the channel protein (Fig. 1e). A single clone was selected from each target. The mutants carried either homozygous insertions (M3KO-1, M3KO-3) or a homozygous deletion (M3KO-2) of single thymidines leading to frameshifts and premature stops within the TRPM3 reading frame. Accordingly, TRPM3 proteins were no longer detectable in the mutants (Fig. 3b). Already in the absence of any stimulus, we observed reduced basal $[Ca^{2+}]_{cyt}$ in *Trpm3* knockout cells (Fig. 3c), indicating that TRPM3 channels may contribute to a constitutive elevation of $[Ca^{2+}]_{cyt}$. None of the *Trpm3* knockout cells displayed elevated $[Ca^{2+}]_{cyt}$ levels in response to PS (Fig. 3c), demonstrating that PS selectively activates TRPM3 channels but no TRPM3-independent Ca^{2+} entry pathways including CaVs. Consistently, TRPM3 currents were no longer detectable in the knockout cells after addition of PS (Fig. 3d, e). Likewise, *Trpm3* knockout cells did not longer show increased insulin levels after PS application, confirming that the PS-induced insulin release of INS-1 cells exclusively depends on TRPM3 (Fig. 3f).

TRPM3 channels contribute to glucose-stimulated insulin release in INS-1 cells

We next asked, whether TRPM3 channels in beta cells are stimulated by glucose and if so, whether TRPM3 activity contributes to glucose-induced insulin release? To answer this question, we performed Ca^{2+} measurements using wild-type and TRPM3-deficient INS-1 cells (Fig. 4a, b). Again, in the absence of glucose, we observed reduced basal $[Ca^{2+}]_{cyt}$ in the knockout cells. In the presence of 20 mM glucose, Ca^{2+} oscillations and the mean cytosolic Ca^{2+} concentration significantly increased in wild-type cells over a period of ~20 min with a delay of ~2-3 min before it decreased again slowly (Fig. 4a, b). In contrast, in *Trpm3* knockout cells, the glucose-induced increase of $[Ca^{2+}]_{cyt}$ was strongly reduced, showing that glucose activates TRPM3 channels in pancreatic beta cells. Correspondingly, we found the glucose-dependent insulin release significantly reduced in all three independent *Trpm3* knockout clones (Fig. 4c). This finding clearly demonstrates the contribution of TRPM3 channels to glucose-induced insulin release from beta cells.

TRPM3-deficient mice display a delayed clearance of blood glucose in response to a glucose load

Does this result also apply to TRPM3 channels in beta cells of whole organisms? If this would be the case, one would expect that in animals lacking TRPM3 channels blood sugar levels decrease much slower after glucose ingestion due to reduced insulin release. To analyse this question, we generated mice lacking TRPM3 channels exclusively in pancreatic beta cells (beta cell-specific *Trpm3* knockout) using a Cre-loxP strategy (Fig. 5a). Mice carrying two floxed *Trpm3* alleles each with the channel pore-forming exon 24 flanked by loxP sequences (*Trpm3^{fllox/fllox}*) were mated with mice in which one *Trpm3* allele was deleted and which additionally carried a Cre recombinase transgene under the control of the rat insulin promoter (*Trpm3^{+/-}*, RIP-Cre⁺, [32]). The *Trpm3^{-/fllox}*, RIP-Cre⁺ offspring lacked both TRPM3 alleles exclusively in beta cells due to insulin promoter-driven Cre recombinase expression. These *Trpm3^{-/fllox}*, RIP-Cre⁺ animals were compared to their *Trpm3^{-/fllox}*, RIP-Cre⁻ littermates lacking the transgene (control). There was no difference in resting blood glucose levels before the application of glucose (Fig. 5b, c). However, *Trpm3^{-/fllox}*, RIP-Cre⁺ mice displayed a delayed glucose clearance 60 min after administration of glucose compared to the controls. This difference was apparent in adult animals after oral administration of glucose (Fig. 5b) as well as after intraperitoneal application of glucose (Fig. 5c). In summary, the data indicate that TRPM3 channels contribute *in vivo* to glucose clearance most probably by increasing the glucose-induced insulin release from beta cells.

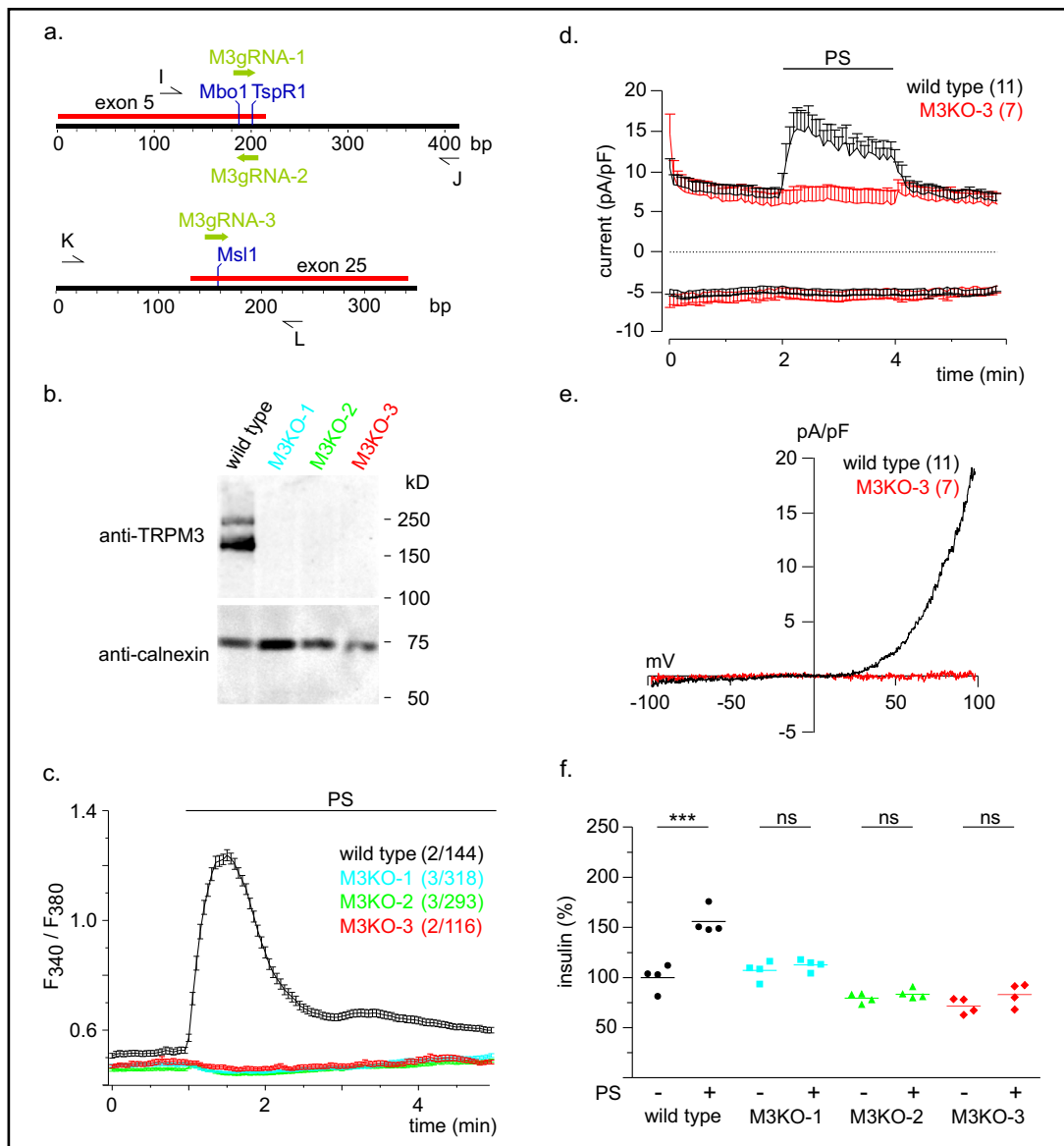


Fig. 3. Absence of PS-induced $[Ca^{2+}]_{cyt}$ elevations, ionic currents, and insulin release in TRPM3-deficient INS-1 cells. (a) CRISPR/Cas9-based strategy for the deletion of the *Trpm3* gene. The locations of the target sequences for the guide RNAs M3gRNA-1, M3gRNA-2, and M3gRNA-3, of the restriction enzymes Mbo1, TspR1, and Msl1 to analyse introduced mutations and of the oligonucleotide primers I, J, K, and L to amplify genomic sequences are indicated. (b) Absence of TRPM3 in the mutant INS-1 cell clones M3KO-1, M3KO-2, and M3KO-3. TRPM3 proteins from wild-type as well as from mutant INS-1 cells were precipitated using polyclonal anti-TRPM3 antibodies and detected on a western blot (upper panel) with monoclonal anti-TRPM3 antibodies. A western blot of non-precipitated proteins (lower panel) was incubated with anti-calnexin antibodies to detect calnexin as loading control. (c) Fura-2 fluorescence ratios observed in wild-type and mutant INS-1 cell clones before and after addition of 100 μM PS. Traces represent mean values (\pm SEM) with the numbers of experiments/cells indicated in brackets. (d) Whole-cell in- and outward currents normalized to the cell size (pA/pF) at -80 and 80 mV, respectively, were extracted from voltage ramps (0.5 Hz) spanning from -100 to 100 mV within 400 ms (V_h 0 mV) and plotted versus time in wild-type cells (black) and the TRPM3-deficient M3KO-3 clone (red) in the presence or absence of 100 μM PS. Experiments were performed in the presence of 10 μM verapamil to block L-type Ca^{2+} channels. Data represent means (\pm S.E.M.) of the cell number indicated in brackets. (e) Current-voltage relationships (IVs) of the mean maximum net currents ($I_{max, net}$) shown in d during the application of PS. (f) Insulin released from wild-type INS-1 cells and *Trpm3* knockout INS-1 cell clones M3KO-1, M3KO-2, and M3KO-3 in the absence (-) or presence (+) of 100 μM PS. Values were normalized to the mean level obtained in wild-type cells without PS.

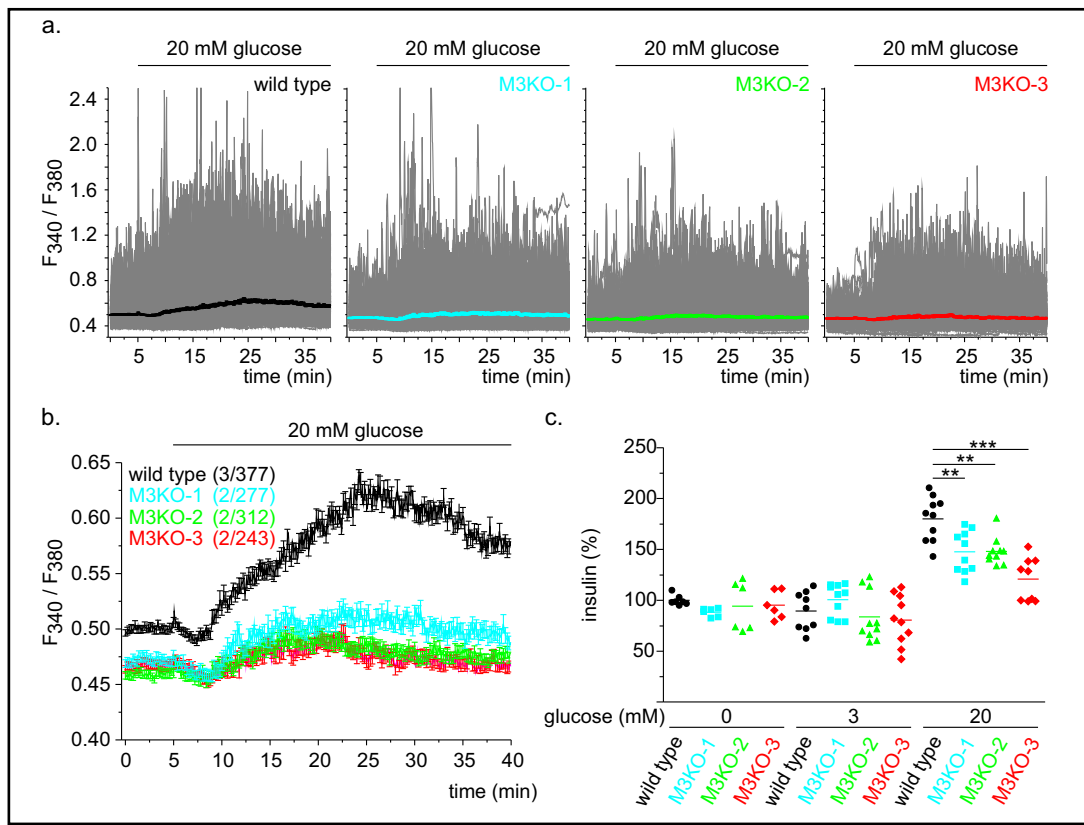


Fig. 4. Reduced glucose-induced increase of $[Ca^{2+}]_{cyt}$ and insulin release in *Trpm3* knockout cells. (a) Fura-2 fluorescence ratios recorded in INS-1 cells before and after addition of 20 mM glucose in wild type and the TRPM3-deficient INS-1 cell clones M3KO-1, M3KO-2, and M3KO-3. Measurements of single cells are shown as thin grey traces. Thick traces represent the mean values (\pm SEM), compared in (b) with numbers of experiments/cells indicated in brackets. (c) Insulin released from wild-type INS-1 cells and *Trpm3* knockout INS-1 cell clones in the absence and presence of 3 and 20 mM glucose. Values were normalized to the mean level obtained in wild-type cells in the absence of glucose. Note that all values in 20 mM glucose were significantly different from the corresponding values in 0 mM and 3 mM glucose with $p < 0.001$ whereas values in 0 and 3 mM glucose were not statistically different from each other.

Discussion

TRPM3 channels trigger insulin release both independently and in concert with CaV channels

In agreement with previous reports, we show here in pancreatic beta cells of the line INS-1 that both, Ca^{2+} entry into the cell and insulin released by the cell are increased after the addition of the TRPM3 agonist PS [22, 33]. By comparison of wild-type and *Trpm3* knockout cells, we also demonstrate that the PS-induced Ca^{2+} signal and the PS-induced insulin release are initiated exclusively via TRPM3 channels and that verapamil effectively inhibits CaVs but not TRPM3 channels. In the presence of high concentrations of verapamil sufficient to block CaVs, PS still substantially increased not only cytosolic Ca^{2+} levels but also the release of insulin, demonstrating that Ca^{2+} entering the cells through TRPM3 channels is in principle sufficient to trigger the insulin release independently of other Ca^{2+} entry pathways. Consequently, we found that most of the transcripts that are expressed in INS-1 cells encoded a Ca^{2+} -permeable pore. At physiological ion concentrations, TRPM3 isoforms with such a pore loop display a fractional Ca^{2+} current of 24 % [9] and are therefore expected to substantially raise $[Ca^{2+}]_{cyt}$. However, we still found a pronounced effect of verapamil on both the PS-induced Ca^{2+} signals

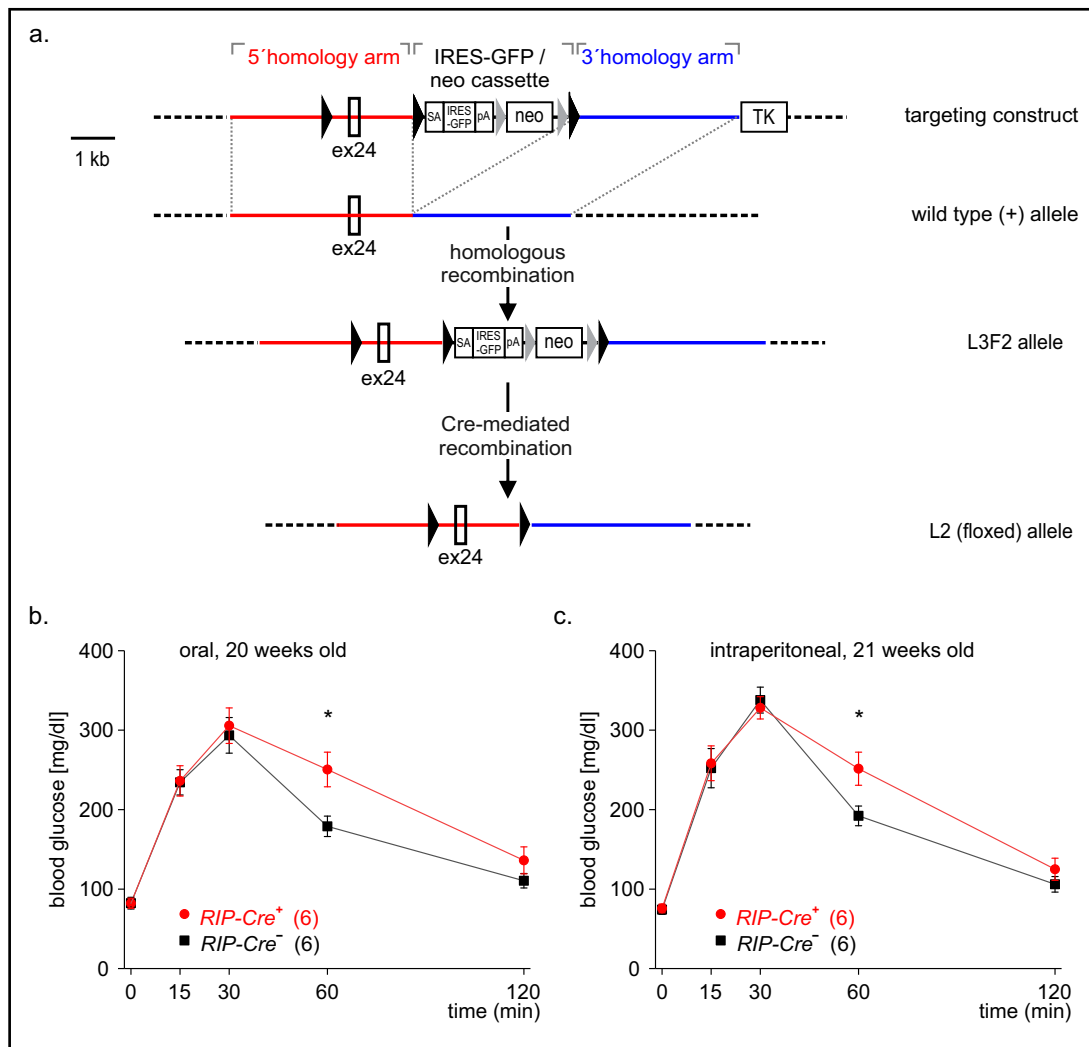


Fig. 5. Impaired glucose clearance in TRPM3-deficient mice. (a) Targeted disruption of the mouse *Trpm3* gene by the introduction of loxP sites flanking the pore coding exon 24 (ex 24). The targeting construct contained three loxP sites (filled black triangles), a 5' homology arm (including ex24), a splice acceptor site (SA), an internal ribosome entry site (IRES), the cDNA of the enhanced green fluorescent protein (GFP), a polyadenylation signal (PA), two flippase recognition targets (grey triangles), a neomycin resistance gene (neo), a 3' homology arm and a herpes simplex virus thymidine kinase cassette (TK). Homologous recombination with the wild-type (+) *Trpm3* allele yielded a modified L3F2 allele and subsequent Cre-mediated recombination produced an L1 (-) allele lacking exon 24 (*Trpm3* knockout) as described in [15] (not shown) as well as a fully functional L2 allele with loxP sites flanking exon 24 (floxed allele). (b, c) Glucose tolerance tests in *Trpm3*^{/floxed} mice carrying a transgene encoding the Cre recombinase under the control of the rat insulin promoter (*RIP-Cre*⁺, red labels) and their littermates lacking this transgene (*RIP-Cre*⁻, black labels). Measurements were performed before (0 min) and 15, 30, 60, and 120 min after oral (b) or intraperitoneal (c) application of glucose in 20 or 21 weeks old mice, respectively. The numbers of individuals tested are indicated in brackets.

and the PS-induced insulin secretion proving an indirect contribution of CaVs to PS-induced signalling pathways in INS-1 cells. This indirect contribution is attributed to a TRPM3-controlled increase of the membrane potential that raises the open probability of CaVs (Fig. 6). This leads to additional Ca²⁺ entry into the cells and therefore to enhanced insulin release. TRPM3 might interfere with the oscillatory change of the membrane potential similar to what has been shown for Ca²⁺ impermeable TRPM5 channels [3]. In contrast to Ca²⁺-impermeable

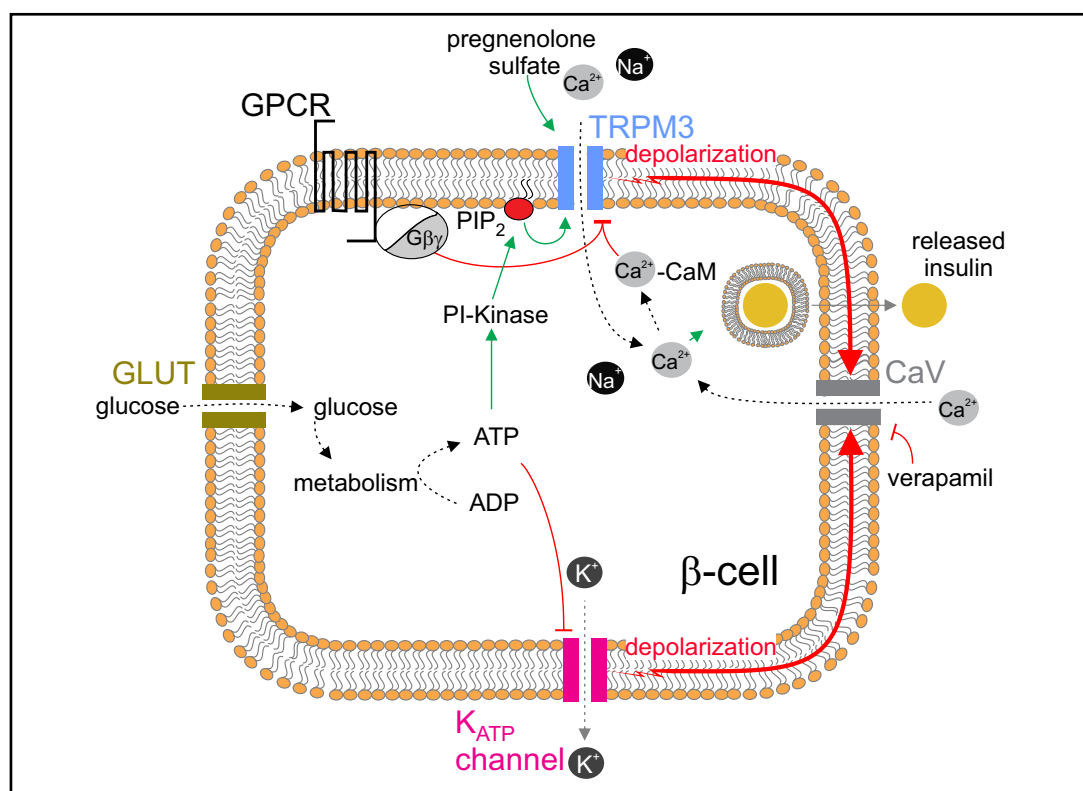


Fig. 6. Contribution of TRPM3 channels to Ca²⁺ entry and insulin release in beta cells. Opening of TRPM3 channels after binding of the TRPM3 agonist pregnenolone sulfate promotes Ca²⁺ and Na⁺ influx and membrane depolarization which in turn triggers additional Ca²⁺ entry into the cell through verapamil-sensitive CaV channels resulting in the release of insulin. Glucose taken up by glucose transporters (GLUT) and metabolized in the cell increases the amount of ATP which blocks ATP-sensitive potassium (K⁺) channels (K_{ATP} channels). Their closure leads to membrane depolarization and the opening of CaVs. Independent of PS, glucose triggers TRPM3 activity conceivably via ATP-dependent activation of phosphatidylinositol-kinase (PI-Kinase), regeneration of phosphatidylinositol 4,5-bisphosphate (PIP₂), and direct PIP₂-mediated stimulation of TRPM3. TRPM3 activity is suppressed by direct interaction with Gβγ-subunits of G-protein coupled receptors (GPCR) as well as Ca²⁺/calmodulin (CaM).

TRPM5 channels, TRPM3 channels may also directly interfere with the oscillatory change of [Ca²⁺]_{cyt} because of their own Ca²⁺ permeability.

In line with this scenario, we observed reduced Ca²⁺ oscillations in all TRPM3-deficient INS-1 clones. Thus, we suggest a constitutive TRPM3 activity in wild-type INS-1 beta cells as it has been described for overexpressed TRPM3 channels as well as for native TRPM3 channels in vascular smooth muscle cells [6-8, 37]. We suggest that constitutive TRPM3 activity fine-tunes the basal [Ca²⁺]_{cyt} and contributes to the regulation of the membrane potential. Constitutive TRPM3 activity may therefore increase the probability for CaV channel openings also in the absence of any external stimuli. Accordingly, we found that the CaV channel blocker verapamil reduced basal [Ca²⁺]_{cyt} already in the absence of external stimuli. Isosakuranetin did not change basal [Ca²⁺]_{cyt} since this flavanone conceivably acts as competitive antagonists of PS that -in contrast to inverse agonists- do not affect constitutive TRPM3 activity.

TRPM3 channels participate in glucose-stimulated insulin secretion

The application of PS uncovered the potential of TRPM3 channels to trigger the release of insulin from INS-1 cells. However, reliable data about the incidence and concentration of PS in the endocrine pancreas are lacking and hitherto there is no experimental evidence

for an involvement of PS in the control of insulin release. Therefore, we asked whether TRPM3 channels also respond to glucose – the most important trigger of insulin release. Our data demonstrate a significant reduction of the glucose-induced insulin release in TRPM3-deficient beta cell clones. Accordingly, glucose-induced Ca^{2+} oscillations were strongly decreased in the absence of TRPM3 channels. Thus, TRPM3 channels do not only increase the insulin release in response to direct and extracellular binding of PS [5] but also in response to elevated levels of glucose (Fig. 4). In line with our finding Klose and co-workers showed that the TRPM3 antagonist mefenamic acid attenuated glucose-stimulated insulin secretion from INS-1 cells [33]. These results are now further supported by our investigations of blood sugar levels *in vivo*. Similar to recent observations made in mice with a global TRPM3 deficiency [10], beta cell-specific *Trpm3* knockout mice showed no differences in resting blood glucose levels, indicating that basal insulin release is not substantially influenced by TRPM3. However, after oral as well as after intraperitoneal glucose administration we found a delayed clearance of blood glucose in mice lacking TRPM3 channels in pancreatic beta cells 60 min after glucose load. This observation strongly indicates that TRPM3 channels contribute to glucose clearance *in vivo* and further supports the finding that TRPM3 channels participate in glucose-stimulated insulin secretion. In apparent contradiction to these findings, Held and co-workers did not observe significant differences in insulin release from isolated Langerhans islets from wild-type mice and mice with a global *Trpm3*-deficiency 15 min after stimulation with 20 mM glucose [22]. The reason for this discrepancy is not known but might be related to different time intervals of the observations. Also, differences between wild-type mice and mice with a global *Trpm3*-deficiency may have been covered by compensatory mechanisms not related to beta cell function.

It remains an open question, how increased glucose levels influence TRPM3-mediated Ca^{2+} entry and insulin release. Similar to the closure of ATP-sensitive potassium channels (K_{ATP} channels) by ATP, we suggest a mechanism that couples metabolic changes following glucose uptake to the electrical activity of the cell (Fig. 6). Like for K_{ATP} channels, this may depend on secondary mediators that are built by catabolism of glucose. For TRPM2 cyclic adenosine diphosphate-ribose and nicotinamide adenine dinucleotide has been proposed as such mediator [4]. For TRPM3, convincing evidence for direct regulation by different membrane phosphatidylinositol phosphates has been provided after heterologous TRPM3 expression [16, 17] as well as in INS-1 cells [16].

Thus increased ATP-levels resulting from glucose catabolism may not only reduce the open probability of K_{ATP} channels but may also increase at first the PI-Kinase activity, thereby the amount of phosphoinositides (like PIP_2) in the plasma membrane and finally the TRPM3 activity linking TRPM3 channels to PIP_2 -mediated control of Ca^{2+} influx and signalling pathways which shape insulin release [38-40] (Fig. 6). We assume additional regulatory mechanisms to be involved. The TRPM3 channel activity is strongly inhibited by intracellular Ca^{2+} conceivably mediated by the Ca^{2+} binding protein calmodulin (CaM, [18, 19]) and it has been reported that “ PIP_2 interacts with CaM binding domains on TRPM3 N-terminus” [20] (Fig. 6). As described in neurons, G-protein coupled receptors (GPCR) may inhibit TRPM3 activity and may link TRPM3 to sympathoadrenal input to reduce insulin release and increase blood glucose levels under stress conditions (Fig. 6).

Similar to INS-1 cells, the *Trpm3* gene is expressed in human primary pancreatic beta cells [41] and we assume that TRPM3 channels might serve similar functions in human beta cells. However, future investigations need to confirm whether TRPM3 channels indeed participate in glucose-stimulated insulin secretion in humans. Interestingly, prediabetes and type 2 diabetes mellitus were found to be inversely related to the serum concentration of the PS-precursor pregnenolone in the Chinese rural population [42] and PS levels were shown to be selectively increased during insulin-induced hypoglycaemia [43].

Conclusion

In conclusion, our results suggest an essential role of TRPM3 channels in the control of glucose-dependent insulin release and therefore open up TRPM3 channels as new targets for the development of antidiabetic drugs.

Acknowledgements

INS-1 cells were a generous gift from Per-Olof Berggren and Barbara Leibiger, Karolinska Institutet, Stockholm. We thank Veit Flockerzi and Johannes Oberwinkler for helpful discussions and critically reading the manuscript and Ute Soltek, Heidi Löhr and Martin Simon-Thomas for excellent technical help.

Author Contributions

A. Becker, S. Mannebach and S.E. Philipp designed research. A. Becker, S. Mannebach, I. Mathar, A.P. Loodin, C. Fecher-Trost, A. Beck and S.E. Philipp performed experiments. A. Becker, S. Mannebach, P. Weissgerber, M. Freichel, A. Belkacemi, A. Beck and S.E. Philipp analysed data. M. Freichel edited the paper. A. Becker co-wrote the paper. S.E. Philipp wrote the paper.

Funding Sources

This work was supported by grants from the Deutsche Forschungsgemeinschaft (DFG, German Research Foundation) CRC 894 (P. Weissgerber, A. Beck, S.E. Philipp), CRC 1118 (M. Freichel) and the Universität des Saarlandes (HOMFOR, S.E. Philipp).

We acknowledge support by the Deutsche Forschungsgemeinschaft (DFG, German Research Foundation) and Saarland University within the funding programme Open Access Publishing.

Statement of Ethics

The authors have no ethical conflicts to disclose.

Disclosure Statement

The authors have no conflicts of interest to declare.

References

- 1 Yang SN, Shi Y, Yang G, Li Y, Yu J, Berggren PO: Ionic mechanisms in pancreatic beta cell signaling. *Cell Mol Life Sci* 2014;71:4149-4177.
- 2 Philippaert K, Vennekens R. The Role of TRP Channels in the Pancreatic Beta-Cell. In: Emir TLR (ed): *Neurobiology of TRP Channels*. Frontiers in Neuroscience. Boca Raton (FL): CRC Press/Taylor & Francis, 2017, pp 229-250.
- 3 Colsoul B, Schraenen A, Lemaire K, Quintens R, Van Lommel L, Segal A, Owsianik G, Talavera K, Voets T, Margolskee RF, Kokrashvili Z, Gilon P, Nilius B, Schuit FC, Vennekens R: Loss of high-frequency glucose-induced Ca²⁺ oscillations in pancreatic islets correlates with impaired glucose tolerance in *Trpm5*^{-/-} mice. *Proc Natl Acad Sci U S A* 2010;107:5208-5213.
- 4 Uchida K, Dezaki K, Damdindorj B, Inada H, Shiuchi T, Mori Y, Yada T, Minokoshi Y, Tominaga M: Lack of TRPM2 impaired insulin secretion and glucose metabolisms in mice. *Diabetes* 2011;60:119-126.
- 5 Wagner TF, Loch S, Lambert S, Straub I, Mannebach S, Mathar I, Dufer M, Lis A, Flockerzi V, Philipp SE, Oberwinkler J: Transient receptor potential M3 channels are ionotropic steroid receptors in pancreatic beta cells. *Nat Cell Biol* 2008;10:1421-1430.

- 6 Grimm C, Kraft R, Sauerbruch S, Schultz G, Harteneck C: Molecular and functional characterization of the melastatin-related cation channel TRPM3. *J Biol Chem* 2003;278:21493-21501.
- 7 Lee N, Chen J, Sun L, Wu S, Gray KR, Rich A, Huang M, Lin JH, Feder JN, Janovitz EB, Levesque PC, Blonar MA: Expression and characterization of human transient receptor potential melastatin 3 (hTRPM3). *J Biol Chem* 2003;278:20890-20897.
- 8 Oberwinkler J, Lis A, Giehl KM, Flockerzi V, Philipp SE: Alternative splicing switches the divalent cation selectivity of TRPM3 channels. *J Biol Chem* 2005;280:22540-22548.
- 9 Drews A, Loch S, Mohr F, Rizun O, Oberwinkler J: The fractional calcium current through fast ligand-gated TRPM channels. *Acta Physiol* 2010;198:P-TUE-115.
- 10 Vriens J, Owsianik G, Hofmann T, Philipp SE, Stab J, Chen X, Benoit M, Xue F, Janssens A, Kerselaers S, Oberwinkler J, Vennekens R, Gudermann T, Nilius B, Voets T: TRPM3 is a nociceptor channel involved in the detection of noxious heat. *Neuron* 2011;70:482-494.
- 11 Vandewauw I, De Clercq K, Mulier M, Held K, Pinto S, Van Ranst N, Segal A, Voet T, Vennekens R, Zimmermann K, Vriens J, Voets T: A TRP channel trio mediates acute noxious heat sensing. *Nature* 2018;555:662-666.
- 12 Dembla S, Behrendt M, Mohr F, Goecke C, Sondermann J, Schneider FM, Schmidt M, Stab J, Enzeroth R, Leitner MG, Nunez-Badinez P, Schwenk J, Nürnberg B, Cohen A, Philipp SE, Greffrath W, Bünemann M, Oliver D, Zakharian E, Schmidt M, et al.: Anti-nociceptive action of peripheral mu-opioid receptors by G-beta-gamma protein-mediated inhibition of TRPM3 channels. *Elife* 2017;6:e26280.
- 13 Badheka D, Yudin Y, Borbiro I, Hartle CM, Yazici A, Mirshahi T, Rohacs T: Inhibition of Transient Receptor Potential Melastatin 3 ion channels by G-protein betagamma subunits. *Elife* 2017;6:e26147.
- 14 Quallo T, Alkhatib O, Gentry C, Andersson DA, Bevan S: G protein betagamma subunits inhibit TRPM3 ion channels in sensory neurons. *Elife* 2017;6:e26138.
- 15 Alkhatib O, da Costa R, Gentry C, Quallo T, Mannebach S, Weissgerber P, Freichel M, Philipp SE, Bevan S, Andersson DA: Promiscuous G-Protein-Coupled Receptor Inhibition of Transient Receptor Potential Melastatin 3 Ion Channels by G β Subunits. *J Neurosci* 2019;39:7840-7852.
- 16 Toth BI, Konrad M, Ghosh D, Mohr F, Halaszovich CR, Leitner MG, Vriens J, Oberwinkler J, Voets T: Regulation of the transient receptor potential channel TRPM3 by phosphoinositides. *J Gen Physiol* 2015;146:51-63.
- 17 Badheka D, Borbiro I, Rohacs T: Transient receptor potential melastatin 3 is a phosphoinositide-dependent ion channel. *J Gen Physiol* 2015;146:65-77.
- 18 Przibilla J, Dembla S, Rizun O, Lis A, Jung M, Oberwinkler J, Beck A, Philipp SE: Ca⁽²⁺⁾-dependent regulation and binding of calmodulin to multiple sites of Transient Receptor Potential Melastatin 3 (TRPM3) ion channels. *Cell Calcium* 2018;73:40-52.
- 19 Holakovska B, Grycova L, Jirku M, Sulc M, Bumba L, Teisinger J: Calmodulin and S100A1 interact with N-terminus of TRPM3 channel. *J Biol Chem* 2012;287:16645-16655.
- 20 Holendova B, Grycova L, Jirku M, Teisinger J: PtdIns(4,5)P2 interacts with CaM binding domains on TRPM3 N-terminus. *Channels* 2012;6:479-482.
- 21 Wagner TF, Drews A, Loch S, Mohr F, Philipp SE, Lambert S, Oberwinkler J: TRPM3 channels provide a regulated influx pathway for zinc in pancreatic beta cells. *Pflugers Arch* 2010;460:755-765.
- 22 Held K, Kichko T, De Clercq K, Klaassen H, Van Bree R, Vanherck JC, Marchand A, Reeh PW, Chaltin P, Voets T, Vriens J: Activation of TRPM3 by a potent synthetic ligand reveals a role in peptide release. *Proc Natl Acad Sci U S A* 2015;112:E1363-1372.
- 23 Asfari M, Janjic D, Meda P, Li G, Halban PA, Wollheim CB: Establishment of 2-mercaptoethanol-dependent differentiated insulin-secreting cell lines. *Endocrinology* 1992;130:167-178.
- 24 Frühwald J, Camacho Londono J, Dembla S, Mannebach S, Lis A, Drews A, Wissenbach U, Oberwinkler J, Philipp SE: Alternative splicing of a protein domain indispensable for function of transient receptor potential melastatin 3 (TRPM3) ion channels. *J Biol Chem* 2012;287:36663-36672.
- 25 Philipp S, Strauss B, Hirnet D, Wissenbach U, Mery L, Flockerzi V, Hoth M: TRPC3 mediates T-cell receptor-dependent calcium entry in human T-lymphocytes. *J Biol Chem* 2003;278:26629-26638.
- 26 Ran FA, Hsu PD, Wright J, Agarwala V, Scott DA, Zhang F: Genome engineering using the CRISPR-Cas9 system. *Nat Protoc* 2013;8:2281-2308.
- 27 Heigwer F, Kerr G, Boutros M: E-CRISP: fast CRISPR target site identification. *Nat Methods* 2014;11:122-123.

- 28 Bae S, Park J, Kim JS: Cas-OFFinder: a fast and versatile algorithm that searches for potential off-target sites of Cas9 RNA-guided endonucleases. *Bioinformatics* 2014;30:1473-1475.
- 29 Szymczak AL, Vignali DA: Development of 2A peptide-based strategies in the design of multicistronic vectors. *Expert Opin Biol Ther* 2005;5:627-638.
- 30 Fairless R, Beck A, Kravchenko M, Williams SK, Wissenbach U, Diem R, Cavalié A: Membrane potential measurements of isolated neurons using a voltage-sensitive dye. *PLoS One* 2013;8:e58260.
- 31 Lakso M, Pichel JG, Gorman JR, Sauer B, Okamoto Y, Lee E, Alt FW, Westphal H: Efficient *in vivo* manipulation of mouse genomic sequences at the zygote stage. *Proc Natl Acad Sci U S A* 1996;93:5860-5865.
- 32 Ray MK, Fagan SP, Moldovan S, DeMayo FJ, Brunicardi FC: Development of a transgenic mouse model using rat insulin promoter to drive the expression of CRE recombinase in a tissue-specific manner. *Int J Pancreatol* 1999;25:157-163.
- 33 Klose C, Straub I, Riehle M, Ranta F, Krautwurst D, Ullrich S, Meyerhof W, Harteneck C: Fenamates as TRP channel blockers: mefenamic acid selectively blocks TRPM3. *Br J Pharmacol* 2011;162:1757-1769.
- 34 Oberwinkler J, Philipp SE: TRPM3. *Handb Exp Pharmacol* 2014;222:427-459.
- 35 Straub I, Mohr F, Stab J, Konrad M, Philipp SE, Oberwinkler J, Schaefer M: Citrus fruit and fabacea secondary metabolites potently and selectively block TRPM3. *Br J Pharmacol* 2013;168:1835-1850.
- 36 Straub I, Krugel U, Mohr F, Teichert J, Rizun O, Konrad M, Oberwinkler J, Schaefer M: Flavanones that selectively inhibit TRPM3 attenuate thermal nociception *in vivo*. *Mol Pharmacol* 2013;84:736-750.
- 37 Naylor J, Li J, Milligan CJ, Zeng F, Sukumar P, Hou B, Sedo A, Yuldasheva N, Majeed Y, Beri D, Jiang S, Seymour VA, McKeown L, Kumar B, Harteneck C, O'Regan D, Wheatcroft SB, Kearney MT, Jones C, Porter KE, et al.: Pregnenolone sulphate- and cholesterol-regulated TRPM3 channels coupled to vascular smooth muscle secretion and contraction. *Circ Res* 2010;106:1507-1515.
- 38 Zhang J, Luo R, Wu H, Wei S, Han W, Li G: Role of type Ialpha phosphatidylinositol-4-phosphate 5-kinase in insulin secretion, glucose metabolism, and membrane potential in INS-1 beta-cells. *Endocrinology* 2009;150:2127-2135.
- 39 Hao M, Bogan JS: Cholesterol regulates glucose-stimulated insulin secretion through phosphatidylinositol 4,5-bisphosphate. *J Biol Chem* 2009;284:29489-29498.
- 40 Xie B, Nguyen PM, Guček A, Thonig A, Barg S, Idevall-Hagren O: Plasma Membrane Phosphatidylinositol 4,5-Bisphosphate Regulates Ca⁽²⁺⁾-Influx and Insulin Secretion from Pancreatic β Cells. *Cell Chem Biol* 2016;23:816-826.
- 41 Marabita F, Islam MS: Expression of Transient Receptor Potential Channels in the Purified Human Pancreatic beta-Cells. *Pancreas* 2017;46:97-101.
- 42 Jiang J, Liu X, Liu X, Tian Z, Zhang H, Qian X, Luo Z, Wei D, Jin S, Wang C, Mao Z: The effect of progesterone and pregnenolone on diabetes status in Chinese rural population: a dose-response analysis from Henan Rural Cohort. *Eur J Endocrinol* 2019;181:603-614.
- 43 Halama A, Kahal H, Bhagwat AM, Zierer J, Sathyapalan T, Graumann J, Suhre K, Atkin SL: Metabolic and proteomic signatures of hypoglycaemia in type 2 diabetes. *Diabetes Obes Metab* 2019;21:909-919.